DOI: 10.1002/cphc.201000136

Structure of Glancing Incidence Deposited TiO_2 Thin Films as Revealed by Grazing Incidence Small-Angle X-ray Scattering

Lola González-García,[b] Angel Barranco,[b] Adela Muñoz Páez,[b] Agustín R. González-Elipe,[b] Mari-Cruz García-Gutiérrez,*[a] Jaime J. Hernández,[a] Daniel R. Rueda,[a] Tiberio A. Ezquerra,[a] and David Babonneau[c]

For the first time, grazing incidence small-angle X-ray scattering (GISAXS) analysis is used to characterize the morphology of TiO_2 thin films grown by glancing angle physical vapor deposition (GLAD). According to cross-section scanning electron microscopy (SEM) images, the films consist of near isotilted TiO_2 columns of different length and width depending on film thickness. The obtained GISAXS patterns show a characteristic asymmetry with respect to the incidence plane, which is associated with the tilted geometry of the TiO_2 columns. The patterns also show the existence of two populations of columns in these GLAD-TiO_2 films. The population of the thinnest columns appears related to the first grown layer and is common for all the films investigated, while the second population of columns grows with the thickness of the films and has been related to wider columns formed by shadowing at the expense of the initially formed columns.

1. Introduction

Titanium dioxide thin films possess outstanding properties, such as high optical transmittance and refractive index, photoactivity, chemical stability, and so forth, that make them suitable for many technological applications.[1] Regarding film morphologies, the formation of ordered nanorods is important for improving the photocatalytic, photovoltaic or sensor properties of nanostructured TiO_2 thin films.[2,3] Among the various methods available to produce nanostructured thin films a very versatile procedure is the use of glancing angle physical vapor deposition (GLAD).[4,5] This method produces porous thin films formed by columns tilted by a certain angle with respect to the substrate. Although different methods of characterization have been used to ascertain the morphology of this type of thin films, to our knowledge grazing incidence small-angle X-ray scattering (GISAXS) [6,7] has not yet been applied. Herein we report on the GISAXS analysis of TiO_2 thin films prepared by GLAD. One of the advantages of GISAXS is the ability to provide averaged statistical information over the entire illuminated sample area, as well as the ability to access buried structures located well below the surface[8] that are not accessible to local probe techniques like scanning electron microscopy (SEM) or atomic force microscopy (AFM). We found that the GLAD thin films give rise to a new kind of asymmetric GISAXS patterns that may result from a morphological evolution of the columns across the thickness of the films. The data analysis also shows that the GISAXS technique is a powerful tool to describe the nanostructure of this kind of thin films.

Experimental Section

TiO_2 thin films were prepared by GLAD at room temperature on silicon substrates. Evaporation was carried out in an electron bombardment evaporator, using TiO pellets as a target. Stoichiometric and columnar thin films of TiO_2 were obtained by evaporation at 10^{-4} torr O_2, placing the substrates at a glancing angle of 80° with respect to the evaporation source. Si-substrates (rectangular pieces of about 1×4 cm^2) were positioned with the shortest edge parallel to the vapor flow direction. Films with thicknesses between 45 nm and 600 nm were prepared.

The microstructure of the TiO_2 thin films deposited on a silicon wafer was examined by field emission scanning electron microscopy (FESEM) in a Hitachi S5200 microscope.

GISAXS experiments were performed at the BW4 beamline (HASYLAB, Hamburg) using a wavelength of $\lambda=0.138$ nm and a sample-to-detector distance of 2.175 m. A moderate microbeam focusing was achieved using beryllium compound refractive lenses (beam size 42×22 µm^2). The scattering signal was recorded with a 2D detector (MAR CCD camera with 79 µm^2 pixel size).

[a] Dr. M.-C. García-Gutiérrez, J. J. Hernández, Dr. D. R. Rueda, Prof. T. A. Ezquerra
Instituto de Estructura de la Materia, CSIC
Serrano 121, 28006 Madrid (Spain)
Fax: (+34) 915645557
E-mail: maricruz@iem.cfmac.csic.es

[b] L. González-García, Dr. A. Barranco, Dr. A. M. Páez, Prof. A. R. González-Elipe
Instituto de Ciencia de Materiales de Sevilla
CSIC—Universidad de Sevilla
Avda. Américo Vespucio 49, 41092 Sevilla (Spain)

[c] Dr. D. Babonneau
Institut P', UPR 3346 CNRS
Université de Poitiers, SP2MI
Bvd M. et P. Curie, BP 30179
86962 Futuroscope Chasseneuil Cedex (France)

2. Results and Discussion

SEM cross-section views of the samples investigated were obtained by cleaving the silicon substrates in the direction parallel to the shortest edge. Figure 1 shows a cross-section view of

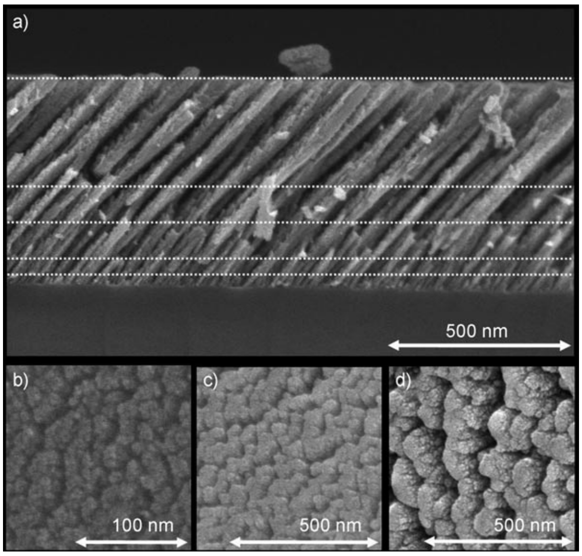

Figure 1. Top: Cross-section SEM micrograph of a) a 600 nm thick TiO_2 film. Bottom: Top-view SEM micrographs of TiO_2 thin films of b) 45, c) 200, and d) 600 nm thickness. The dashed lines plotted in the cross-section view define the height of the thin films used for analysis (i.e. 45, 100, 200, 300, and 600 nm).

a 600 nm TiO_2 film together with a series of normal views of thin films of increasing thickness, as indicated. The cross-section image shows the typical tilted columnar morphology of metal oxide thin films grown by GLAD. The angle between the columns and the substrate surface is around 50°, which is in good agreement with that estimated by employing the simple models proposed to describe the microstructure of this kind of thin films.[5] A close look at this cross-section view also reveals that the diameter of the columns and the distance between them increase towards the surface. This feature is in agreement with the fact that the growth process is dominated by shadow effects.[4,5] Moreover, a high number of short, thinner columns appear in contact with the substrate at the initial stages of the film growth. The increase in the column width with the film thickness is well supported by the top-view images in Figure 1. These top-view images also show that columns grow forming a wavy morphology.

The information extracted from SEM gives qualitative local information, but does not address the internal nanostructure of the films and its variation with the film thickness. To prove the nanostructure of the columnar thin films from the interface to the outer surface over a large area, samples of several square millimeters were investigated by GISAXS. The rectangular sample was aligned horizontally with the long edge parallel to the X-ray beam (x-axis) at a given vertical position (z-axis) to cut only half of the beam intensity. The sample was rotated along the y-axis by selecting a grazing incidence angle, $\alpha_i = 0.4°$. Thus, the primary beam and the reflected beam leave the sample plane, forming an angle of $2\alpha_i$ between them and define the incidence plane (x,z), which intersects the plane detector along the meridian of the GISAXS pattern (see Figure 2).

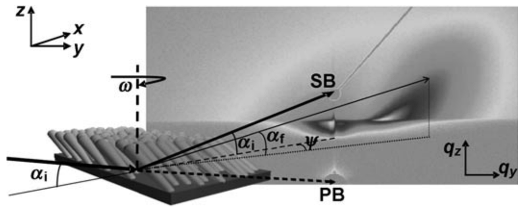

Figure 2. Schematic GISAXS layout showing the geometry used. The sample is positioned with respect to the spatial coordinates x, y, and z as well as by its azimuthal orientation (ω). The sample surface is defined as the xy plane; the incidence plane (xz) containing both the primary beam (PB) and the specular peak (SB) defines the meridian of the GISAXS pattern. The incidence angle is denoted α_i, the exit angle α_f, and the out-of incidence plane angle ψ. The GISAXS pattern corresponds to the 600 nm thick sample.

Each point of a GISAXS pattern is defined by two angular coordinates, ψ and α_f, where ψ is the horizontal angle measured from the meridian or incidence plane and α_f is the vertical exit angle measured from the sample plane. The pattern is also defined by the scattering vector coordinates, q_y and q_z, which can be expressed as functions of the angular coordinates according to the expressions in Equations (1) and (2):

$$q_y = \frac{2\pi}{\lambda}[\sin(\psi)\cos(\alpha_f)] \tag{1}$$

$$q_z = \frac{2\pi}{\lambda}[\sin(\alpha_i) + \sin(\alpha_f)] \tag{2}$$

When the samples investigated with GISAXS are isotropic, that is, have well-aligned scattering objects with an axis of revolution perpendicular to the substrate, the scattered intensity out of the meridian ($q_y \neq 0$) is symmetric with respect to the incidence plane and satisfies the condition in Equation (3):[9]

$$I(-q_y) = I(q_y) \tag{3}$$

In this case, the GISAXS patterns are not sensitive to azimuthal rotation along the z-axis. However, the samples investigated herein show a preferential orientation of the TiO_2 columns with respect to the substrate (see Figure 1). Thus, the GISAXS intensity distribution also depends on the azimuth angle (ω) of the substrate. Moreover, the corresponding GISAXS patterns are asymmetric with respect to the incidence plane. Thus, as shown in Figures 3a–c, if the sample is mounted with the columns tilted to the right, the large and broad scattering appears at the left half where $q_y < 0$, and vice versa; columns tilted to the left scatter mostly to the right half where $q_y > 0$ (Figure 3d). To our knowledge, such patterns have not been reported previously for columnar systems although GISAXS patterns from faceted Ge quantum dots have shown non-centrosymmetric scattering.[7,10,11] Also, it is remarkable that the

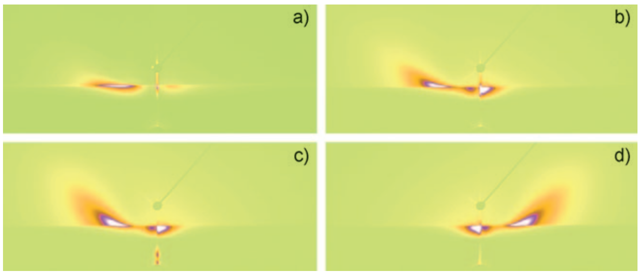

Figure 3. Selected GISAXS patterns for TiO_2 thin films of increasing thickness with the columns tilted to the right: a) 45, b) 300, and c) 600 nm, as well as d) the 600 nm thick sample with the columns tilted to the left.

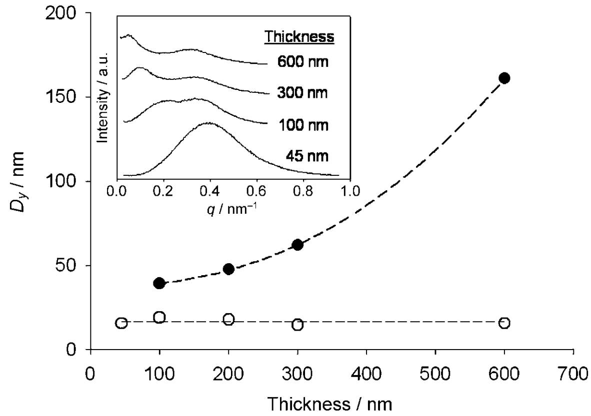

Figure 5. Characteristic lateral lengths obtained from the two GISAXS maxima as a function of sample thickness (●, ○). The dashed lines are a guide for the eye. The inset shows the horizontal intensity profiles of the half of the GISAXS pattern that shows the large scattering.

shape of the intensity distribution is similar for all the samples investigated.

Figure 4 shows that the experimental GISAXS pattern of the thinnest sample can be fairly well reproduced within the distorted-wave Born approximation applied to buried scatterers,[12,13] by means of the FitGISAXS program.[12] We considered a simple model of monodisperse nanocylinders (diameter = 4.8 nm and aspect ratio = 2.7) tilted by 36° with respect to the z-axis, and randomly distributed in a TiO_2 film with 50% porosity. Such a preliminary simulation suggests that the weak intensity present in the right half of the GISAXS pattern could be related to the second order of the form factor, which would reveal that the height distribution of the columns is quite narrow. Next, we focus on the analysis of the half of the GISAXS pattern which shows the large scattering and exhibits only one broad maximum in the case of the thinnest sample. In contrast, the inset in Figure 5, showing horizontal intensity profiles (y-cuts) taken at the q_z value of maximum intensity, illustrates the presence of two scattering maxima in the GISAXS patterns of the TiO_2 samples thicker than 45 nm.

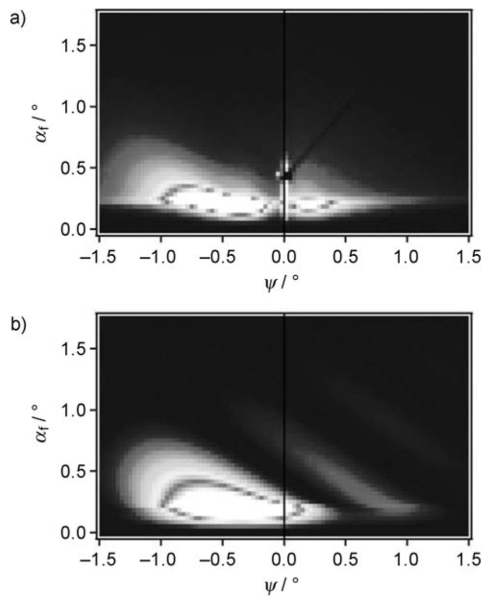

Figure 4. Comparison of the a) experimental and b) simulated GISAXS patterns of the thinnest sample (45 nm). The simulated pattern was determined with the FitGISAXS program.

A first approach to extract quantitative information on the samples investigated is obtained from the position of the scattering maxima (q_y^{max}). The corresponding lateral distance D_y can be derived according to Equation (4):

$$D_y = 2\pi / q_y^{max} \tag{4}$$

Thus, the characteristic lateral lengths derived from the two scattering maxima observed are represented as a function of sample thickness in Figure 5. The broad peak observed for the thinnest sample is still present for the thicker samples (Figure 3) and its position is almost constant, suggesting it to be related to the TiO_2 columns formed at the initial stages of the film growth, as evidenced by the morphology observed below the first dashed line plotted in the cross section SEM image shown in Figure 1. The greater characteristic length (●), which is not observed for the thinnest film (45 nm), presents values in the range of 39–160 nm, increasing with film thickness. This suggests the development of a second population of wider and/or more separated columns that, due to the shadowing effects controlling the growth mechanism of GLAD films,[4,5] grow in length and width at the expense of the initially deposited columns as the thickness of the films increases. This general phenomenology revealed by GISAXS is in agreement with the evolution of the thickness of the columnar microstructure as revealed by the SEM micrographs in Figure 1. Nevertheless, the lateral characteristic length (160 nm) derived for the thickest sample appears to be greater than the inter-column distance revealed by the SEM cross-section image (Figure 1). This discrepancy could be attributed to the influence of the tilting angle of scatters (TiO_2 columns) on the position of GISAXS scattering maxima and/or to the tendency of the GLAD columns to form bundles separated by distances larger than the typical inter-column separation.[4,14]

3. Conclusions

For the first time GISAXS was used to characterize the morphology of TiO_2 thin films grown by GLAD. Because of the tilting of the TiO_2 rods grown on the Si substrate, the obtained GISAXS patterns show a characteristic asymmetry with respect to the meridian or incidence plane. The capability of GISAXS to access buried structures below the surface allowed us to access characteristic lengths which can be assigned to layers with columns of different widths. We anticipate that GISAXS will be a unique technique to elucidate the key parameters of TiO_2 thin films to optimize their photocatalytic, photovoltaic or sensor properties.

Acknowledgements

The authors thank the MICINN (grants MAT 2008–03232, MAT 2009-07789, FPI BES-2006–12807, MAT 2007–65764 and CONSOLIDER INGENIO 2010-CSD2008–00023) and the Junta de Andalucía (project P09-TEP-5283), Spain, for the financial support. The experiments performed at BW4 in HASYLAB (DESY) were supported by the European Community [Contract RII3-CT-2004–506008 (IA-SFS)]. We thank A. Timann for his support during measurements at HASYLAB.

Keywords: GISAXS · GLAD · nanostructures · sensors · thin films

[1] O. Carp, C. L. Huisman, A. Reller, *Prog. Sol. State Ch.* **2004**, *32*, 33 – 177.
[2] G. Centi, S. Perathoner, *Eur. J. Inorg. Chem.* **2009**, *26*, 3851 – 3859.
[3] Y.-Y. Lin, T-H. Chu, Ch-W. Chen, W.-F. Su, *Appl. Phys. Lett.* **2008**, *92*, 053312.
[4] M. M. Hawkeye, M. J. Brett, *J. Vac. Sci. Technol. A* **2007**, *25*, 1317.
[5] C. H. Chang, P. Yu, C. S. Yang, *Appl. Phys. Lett.* **2009**, *94*, 051114.
[6] P. Müller-Buschbaum, *A Basic Introduction to Grazing Incidence Small-Angle X-Ray Scattering*, Lect. Notes Phys. **776**, Springer-Verlag, Berlin, **2009**, **pp.** 61 – 89.
[7] G. Renaud, R. Lazzari, F. Leroy, *Surf. Sci. Rep.* **2009**, *64*, 255 – 380.
[8] D. R. Rueda, A. Nogales, J. J. Hernández, M. C. García-Gutiérrez, T. A. Ezquerra, S. V. Roth, M. G. Zolotukhin, R. Serna, *Langmuir* **2007**, *23*, 12677 – 12681.
[9] T. Salditt, T. H. Metzger, J. Peisl, B. Reinker, M. Moske, K. Samwer, *Europhys. Lett.* **1995**, *32*, 331 – 336.
[10] M. Rauscher, R. Paniago, T. H. Metzger, Z. Kovats, J. Domke, H. D. Pfannes, J. Schulze, I. Eisele, *J. Appl. Phys.* **1999**, *86*, 6763 – 6769.
[11] M.-I. Richard, T. U. Schülli, G. Renaud, E. Wintersberger, G. Chen, G. Bauer, V. Holy, *Phys. Rev. B* **2009**, *80*, 045313.
[12] D. Babonneau, S. Camelio, D. Lantiat, L. Simonot, A. Michel, *Phys. Rev. B* **2009**, *80*, 155446.
[13] D. Babonneau, M. F. Beaufort, A. Declémy, J. F. Barbot, J.P Simon, *J. Appl. Phys.* **2006**, *99*, 113507/1 – 6.
[14] H. van Kranenburg, C. Lodder, *Mater. Sci. Eng. R* **1994**, *11*, 295 – 354.

Received: February 21, 2010
Published online on May 21, 2010

